Research Article
DILI, Autoimmune, Cholestatic and Genetic Diseases

JOURNAL
OF HEPATOLOGY

Inhibition of the renal apical sodium dependent bile acid transporter prevents cholemic nephropathy in mice with obstructive cholestasis

Authors

Ahmed Ghallab, Daniela González, Ellen Strängberg, …, Paul A. Dawson, Erik Lindström, Jan G. Hengstler

Correspondence

ghallab@ifado.de (A. Ghallab), hengstler@ifado.de (J.G. Hengstler).

Graphical abstract

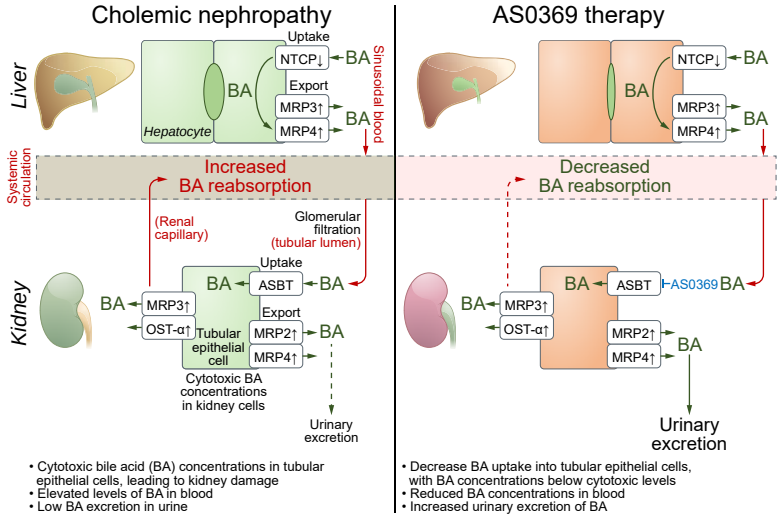

Highlights

- Bile acid enrichment in proximal tubular epithelial cells triggers cholemic nephropathy.
- Blocking renal ASBT prevents bile acid enrichment and death of proximal tubular epithelial cells, thereby preventing cholemic nephropathy.
- Renal ASBT inhibition enhances urinary bile acid excretion and lowers the systemic bile acid pool.
- Renal ASBT expression is preserved in patients with cholemic nephropathy.

Impact and implications

Cholemic nephropathy (CN) is a severe complication of cholestasis and an unmet clinical need. We demonstrate that CN is triggered by the renal accumulation of bile acids (BAs) that are considerably increased in the systemic blood. Specifically, the proximal tubular epithelial cells of the kidney take up BAs via the apical sodium-dependent bile acid transporter (ASBT). We developed a therapeutic compound that blocks ASBT in the kidneys, prevents BA overload in tubular epithelial cells, and almost completely abolished all disease hallmarks in a CN mouse model. Renal ASBT inhibition represents a potential therapeutic strategy for patients with CN.

https://doi.org/10.1016/j.jhep.2023.10.035
 J. Hepatol. 2024, 80, 268–281

Research Article
DILI, Autoimmune, Cholestatic and Genetic Diseases

JOURNAL OF HEPATOLOGY

Inhibition of the renal apical sodium dependent bile acid transporter prevents cholemic nephropathy in mice with obstructive cholestasis

Ahmed Ghallab[1,2,*], Daniela González[1], Ellen Strängberg[3], Ute Hofmann[4], Maiju Myllys[1], Reham Hassan[1,2], Zaynab Hobloss[1], Lisa Brackhagen[1], Brigitte Begher-Tibbe[1], Julia C. Duda[5], Carolin Drenda[5], Franziska Kappenberg[5], Joerg Reinders[1], Adrian Friebel[6], Mihael Vucur[7], Monika Turajski[1], Abdel-latief Seddek[2], Tahany Abbas[8], Noha Abdelmageed[9], Samy A.F. Morad[10], Walaa Morad[8], Amira Hamdy[2], Wiebke Albrecht[1], Naim Kittana[11], Mohyeddin Assali[12], Nachiket Vartak[1], Christoph van Thriel[1], Ansam Sous[12], Patrick Nell[1], Maria Villar-Fernandez[1], Cristina Cadenas[1], Erhan Genc[13], Rosemarie Marchan[1], Tom Luedde[7], Peter Åkerblad[3], Jan Mattsson[3], Hanns-Ulrich Marschall[14,+], Stefan Hoehme[6], Guido Stirnimann[15], Matthias Schwab[4,16,17], Peter Boor[18], Kerstin Amann[19], Jessica Schmitz[20], Jan H. Bräsen[20], Jörg Rahnenführer[5], Karolina Edlund[1], Saul J. Karpen[21], Benedikt Simbrunner[22,23], Thomas Reiberger[22,23], Mattias Mandorfer[22,23], Michael Trauner[22,24], Paul A. Dawson[21,#], Erik Lindström[3,#], Jan G. Hengstler[1,*,#]

Journal of Hepatology **2024**. vol. 80 | 268–281

Check for updates

See Editorial, pages 188–190

Background & Aims: Cholemic nephropathy (CN) is a severe complication of cholestatic liver diseases for which there is no specific treatment. We revisited its pathophysiology with the aim of identifying novel therapeutic strategies.
Methods: Cholestasis was induced by bile duct ligation (BDL) in mice. Bile flux in kidneys and livers was visualized by intravital imaging, supported by MALDI mass spectrometry imaging and liquid chromatography-tandem mass spectrometry. The effect of AS0369, a systemically bioavailable apical sodium-dependent bile acid transporter (ASBT) inhibitor, was evaluated by intravital imaging, RNA-sequencing, histological, blood, and urine analyses. Translational relevance was assessed in kidney biopsies from patients with CN, mice with a humanized bile acid (BA) spectrum, and via analysis of serum BAs and KIM-1 (kidney injury molecule 1) in patients with liver disease and hyperbilirubinemia.
Results: Proximal tubular epithelial cells (TECs) reabsorbed and enriched BAs, leading to oxidative stress and death of proximal TECs, casts in distal tubules and collecting ducts, peritubular capillary leakiness, and glomerular cysts. Renal ASBT inhibition by AS0369 blocked BA uptake into TECs and prevented kidney injury up to 6 weeks after BDL. Similar results were obtained in mice with humanized BA composition. In patients with advanced liver disease, serum BAs were the main determinant of KIM-1 levels. ASBT expression in TECs was preserved in biopsies from patients with CN, further highlighting the translational potential of targeting ASBT to treat CN.
Conclusions: BA enrichment in proximal TECs followed by oxidative stress and cell death is a key early event in CN. Inhibiting renal ASBT and consequently BA enrichment in TECs prevents CN and systemically decreases BA concentrations.

Introduction

Acute kidney injury (AKI) is a frequent complication in patients with liver disease that leads to high morbidity and mortality[1,2] and has several causes, particularly hemodynamic changes, and infections.[1,3] However, an underestimated and increasingly acknowledged[4,5] cause of AKI in liver diseases is cholemic nephropathy (CN),[2,6,7] which describes renal dysfunction together with characteristic renal histological features such as tubular cell injury and Hall's stain-positive bilirubin casts. It has long been known that the risk of AKI is increased in jaundiced patients.[8,9] CN occurs in individuals with liver diseases of different etiologies, including obstructive cholestasis, decompensated cirrhosis/acute-on-chronic liver failure, alcohol-associated hepatitis, and acute liver injury/failure.[2,3] Despite their different etiology, all these disorders are associated with variable degrees of cholestasis. The frequency of CN is likely underestimated in clinical practice since the diagnosis is based on biopsy-proven tubular injury with bilirubin casts. However, kidney biopsies in patients with hepatic dysfunction are often

Keywords: Cholestasis; bile cast nephropathy; kidney injury; bile duct ligation; intravital imaging.
Received 28 March 2023; received in revised form 6 October 2023; accepted 23 October 2023; available online 7 November 2023
* Corresponding authors. Address: Department of Toxicology, Leibniz Research Centre for Working Environment and Human Factors, Technical University Dortmund, Ardeystr. 67, 44139 Dortmund, Germany. Tel.: 0492311084356 (A. Ghallab) or 0492311084348 (J.G. Hengstler).
E-mail addresses: ghallab@ifado.de (A. Ghallab), hengstler@ifado.de (J.G. Hengstler).
+ Deceased
# Indicates shared senior authorship
https://doi.org/10.1016/j.jhep.2023.10.035

not performed because of a high risk of bleeding.[6] Postmortem kidney autopsy studies of patients with decompensated cirrhosis and acute-on-chronic liver failure hospitalized because of AKI showed histologically proven CN in 75% and 25% of the samples, respectively.[10]

Despite the association with cholestasis, the underlying pathophysiological mechanisms of CN remain unclear.[3,6] Common bile duct ligation (BDL) in mice caused renal tubular epithelial cell (TEC) injury and histological as well as functional alterations mimicking human CN, suggesting a pathogenic role of bile acids (BAs).[11] Increasing the hydrophilicity of the BA pool either via norursodeoxycholic acid feeding or farnesoid X receptor knockout ameliorated CN.[12] These findings suggest that elevated circulating BA levels lead to increased glomerular filtration, resulting in elevated renal levels of BAs that are cytotoxic to epithelial cells lining the tubules and collecting ducts. Nevertheless, there is an ongoing debate about the causal role of BAs *vs.* other cholephiles that are increased in cholestasis, such as bilirubin or inflammatory mediators, in the development of CN.[2,13,14]

Here, we used intravital imaging[15,16] to directly observe glomerular filtration and tubular BA reabsorption. We report that massively increased reabsorption of BAs into proximal TECs in cholestasis is critical for CN pathogenesis. Systemic inhibition of the BA uptake carrier apical sodium-dependent BA transporter (ASBT) with the novel compound AS0369 blocked BA uptake from the tubular lumen and shows therapeutic potential for the treatment of CN.

Materials and methods

A detailed description of all methods is provided in the supplementary methods and in the supplementary CTAT table.

Renal biopsies of patients with CN and human serum

Renal biopsies from patients with CN (21) and without CN (11) were collected from two cohorts: Hannover cohort (14 CN and 4 non-CN biopsies), and Erlangen cohort (7 CN and 7 non-CN biopsies; Table S1A). Serum samples of patients with acute and/or chronic liver disease (n = 67) and bilirubin >6 mg/dl undergoing HVPG measurement ± transjugular liver biopsy at the Vienna Hepatic Hemodynamic Lab were selected from a prospective registry with a biobank (Table S1B). Healthy individuals (n = 36) were volunteers from Dortmund (Table S1B). The clinical studies were conducted according to the ethical guidelines of the 1975 Helsinki Declaration and its later amendments as approved by the local ethics committees (no. 1262/2017, 4415, 22-150-D). Informed consent was obtained from all participants.

Mice, induction of obstructive cholestasis, and AS0369 administration

Eight-to-10-week-old male and female C57BL/6N (Janvier Labs, France) or *Cyp2c70*$^{-/-}$ and corresponding C57BL/6J wild-type (Dawson, Karpen Lab) mice were used. All experiments were approved by the local animal welfare committee (LANUV, North Rhine-Westphalia, Germany, application number: 81-02.04.2022.A286). To induce biliary obstruction, as a model for severe cholestasis, the extrahepatic common bile duct was ligated as previously described.[16] A stock formulation of the ASBT inhibitor AS0369 was prepared as a suspension, and doses of 15, 30, 60 and 120 mg/kg b.w. were administered orally by gavage twice daily.

Intravital imaging

Functional intravital imaging of mouse livers and kidneys was performed using a two-photon microscope (Zeiss, Germany) as previously described.[15]

Results

Enhanced uptake of BAs into renal TECs in obstructive cholestasis

To study the mechanisms by which cholestatic liver disease leads to nephropathy, the liver-kidney axis was analyzed time-dependently in mice up to 12 weeks after BDL or sham operation. In agreement with previous studies,[11,12,16] BDL led to excessive accumulation of bile in the gallbladder, transient elevation of plasma transaminases, and to time-dependent elevation of plasma alkaline phosphatase activity (Fig. S1A-C). Histological analysis of the liver showed progressive ductular reaction, leukocyte infiltration, and fibrosis (Fig. S1D). Intravital imaging of the liver after intravenous bolus injection of fluorophore-coupled taurocholic acid (TCA) demonstrated efficient uptake from the sinusoidal blood into hepatocytes within minutes, followed by secretion into the bile canaliculi in control mice. In contrast, TCA remained elevated in the sinusoidal blood of BDL mice during the entire imaging period (Fig. S2; Video S1).

To visualize the transport of BAs in the kidney of mice with obstructive cholestasis, a bolus of the fluorophore-coupled TCA was administered into the tail vein on day 21 after BDL or sham operation, and intravital videos were recorded. In the controls, a transient, very weak increase of TCA-associated fluorescence was quantified in the peritubular capillaries, then in the tubular lumen and the corresponding TEC (Fig. 1A,B; Video S2A). After BDL, the intensity of the TCA signal was higher and remained increased in the peritubular capillaries (Fig. 1A,C; Video S2B). In addition, a strong uptake of TCA via the apical membrane was observed in some TECs, further named type A, while only a minor increase was seen in other TECs, named type B (Fig. 1A, C). Thus, spatio-temporal intravital analysis revealed strongly reduced BA uptake by the liver, consequently higher and persistently increased blood concentrations, enhanced glomerular filtration and enrichment of BAs in TECs after BDL.

To investigate whether these observations could be reproduced without the use of fluorescent markers, a time-resolved comprehensive analysis of endogenous BAs was performed up to 12 weeks after BDL (Fig. 1D). First, TCA, an abundant endogenous BA in mice, was analyzed in liver and kidney tissues by matrix-assisted laser desorption ionization-mass spectrometry imaging (MALDI-MSI). In liver tissue, BDL caused a transient TCA increase on day 1, which decreased thereafter, but remained above control values (Figs 1E,F and S3). In contrast, in the kidneys, a progressive time-dependent increase in endogenous TCA was detected after BDL (Figs 1E,F and Fig. S3). The results of MALDI-MSI were confirmed by liquid chromatography-tandem mass spectrometry analysis of endogenous BAs in tissue homogenate (Fig. 1G). Blood concentrations of BAs were massively increased at all time intervals after BDL (Fig. 1G). Altogether, these data confirm the adaptive response of the liver to cholestatic conditions and suggest an impaired ability of the kidney to adapt.

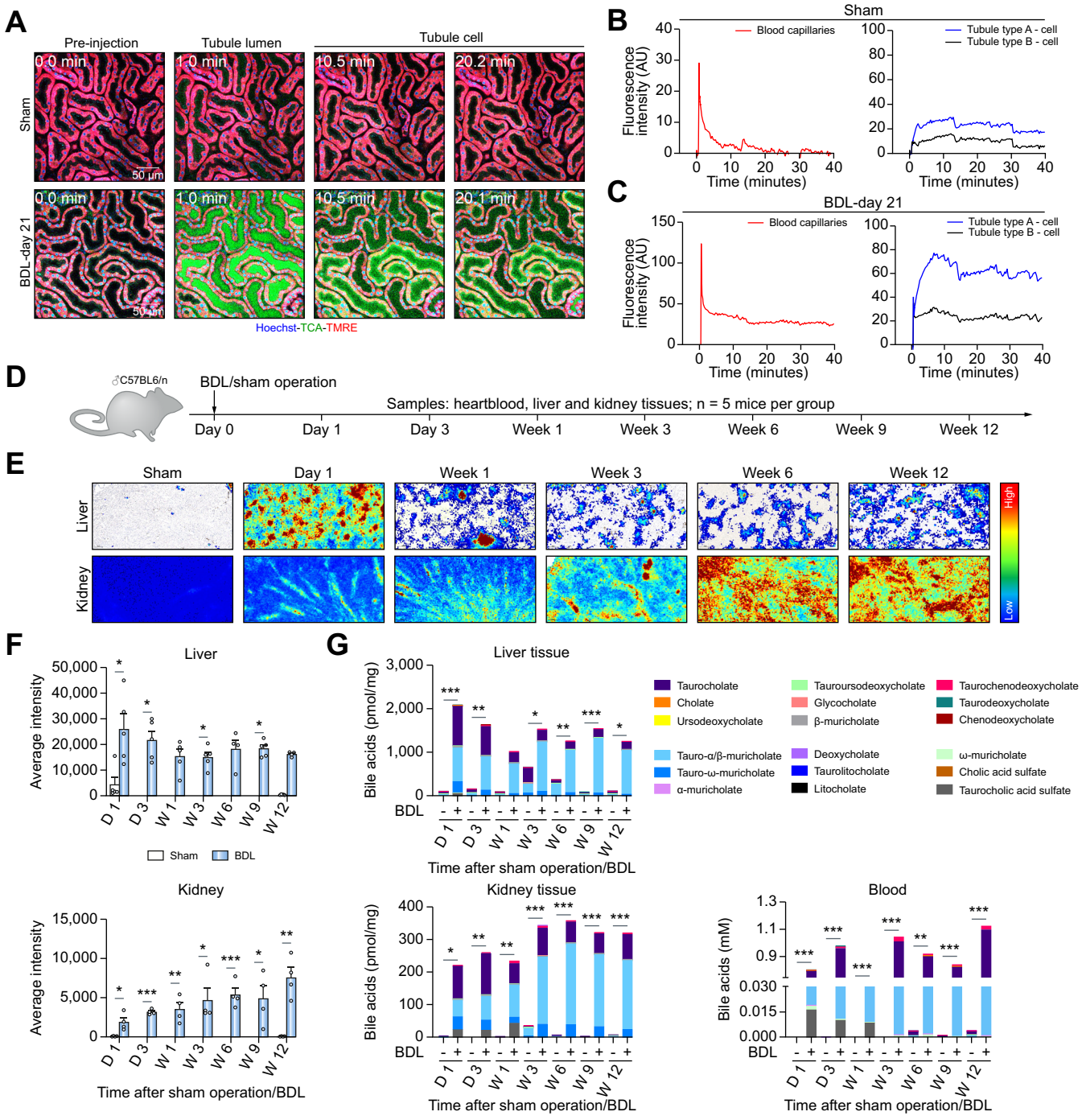

Fig. 1. Enhanced uptake of bile acids into renal tubular epithelial cells in obstructive cholestasis. (A-C) Stills from intravital videos of sham controls and mice 21 days after BDL, and corresponding quantifications. Red: TMRE; green: TCA; blue: Hoechst. Scale bars: 50 µm (Video S2). (D) Experimental schedule. (E,F). MALDI-MSI analysis of mouse livers and kidneys at different time intervals after BDL, and corresponding quantifications. (G) LC-MS/MS analysis of BAs in liver and kidney tissues and in blood; data are presented as mean± SEM; n = 5 mice per group. *p <0.05; **p <0.01; ***p <0.001 compared to sham day 1, Unpaired t test. The data are from male mice. BDL, bile duct ligation; TCA, taurocholic acid; TMRE, tetramethylrhodamine ethyl ester. (This figure appears in color on the web.)

Key events of CN: proximal TEC death and leakiness of peritubular capillaries

To study the consequences of chronic cholestasis on kidney function and morphology, kidney injury biomarkers in blood and urine, and kidney histopathology were analyzed time-dependently after BDL. Urea decreased in urine and increased in blood (Fig. S4A, B). Bilirubin increased in blood and urine of BDL mice compared to controls (Fig. S4A, B). Creatinine concentrations decreased in urine while the urinary output increased (Fig. S4C). Macroscopically, a green discoloration of the kidneys was observed after BDL (Fig. S4D). H&E staining showed tubular cystic dilatation at week 1 after BDL, increasing thereafter, and at week 9 onwards, glomerular cysts were observed. Leukocyte infiltration

and Hall's positive casts occurred 3 days after BDL, with fibrosis appearing at week 6 and intensifying thereafter (Fig. S4D).

To differentiate proximal and distal tubules as well as collecting ducts, kidney tissue was co-immunostained for aquaporin (AQP)1, TSC (thiazide sensitive NaCl cotransporter) and AQP2 (Fig. 2A). Dilatation and casts were observed in the distal tubules and collecting ducts at day 3 and week 1, respectively, but not in proximal tubules. To understand the mechanism of this damage pattern, intravital imaging was performed using the oxidative stress marker H_2DCFDA (Fig. 2B; Fig. S5A). Proximal tubules were differentiated from distal tubules by their higher TMRE (tetramethylrhodamine, ethyl ester) intensity (Fig. S5A, B). As little as 4 h after BDL, oxidative stress was seen specifically in proximal TECs, which intensified until day one. This seemingly contradictory pattern, with dilatation and casts in distal TECs but oxidative stress in proximal TECs was further studied on intravital videos using the cytotoxicity marker SYTOX green and the mitochondrial marker TMRE. Already at day 1 after BDL, death of proximal but not distal TECs occurred (Figs 2C and S5B). The dead proximal TECs released cellular debris into the tubular lumen from where it floated downstream (Fig. 2C; Video S3A). Some of this detritus attached to the surface of distal tubules and collecting ducts forming casts and leading to dilatation (Fig. 2B,C; Video S3A). At week 3 after BDL, massive damage of renal tubules occurred, coinciding with green autofluorescence – possibly due to bilirubin – in and around peritubular capillaries (Figs 2B and S5A). To study if this autofluorescence is due to leaky capillaries, immunostaining of endothelial cells was performed using anti-MECA-32 antibodies. Severely compromised peritubular capillaries were observed particularly at week 3 after BDL and later (Fig. S6A). Intravital imaging was conducted using Evans blue, which under normal conditions does not leak from the capillaries.[17] As expected, Evans blue remained within the blood capillaries in sham-operated mice (Figs 2D,E and S6B; Video S4A). In contrast, 3 weeks after BDL, strong leakage was observed from peritubular capillaries into the interstitium (Figs 2D,E and S6B; Video S4B). At week 12, glomerular cysts manifested as dilatation of Bowman's space (Figs 2B and S5A; Video S3B). The imaging data corresponded to the time course of the proximal TEC marker KIM-1, which increased until week 1 before plateauing and decreasing thereafter (Fig. 2F); the proximal and distal TEC marker neutrophil gelatinase-associated lipocalin (NGAL) remained elevated until the end of the observation period, while the glomerular filtration marker cystatin C increased only at the longest periods of 9 and 12 weeks after BDL (Fig. 2F).

Identification of renal ASBT as a possible therapeutic target in CN

As shown above, BA enrichment in proximal TECs is a key early event in CN progression. The main carrier responsible for reabsorption of the non-sulfated BAs in TECs is ASBT[18] (Fig. 3A). In contrast to the adaptive changes of BA transporters in the liver (Fig. S7), renal *Asbt* expression was not significantly downregulated up to 6 weeks after BDL (Fig. 3B). Renal multidrug resistance-associated protein (MRP)*2*, which pumps BAs into the tubular lumen, was only moderately altered, whereas MRP4, which also exports BAs at the luminal apical membrane, was significantly upregulated (Fig. 3C). Interestingly, the basolateral BA exporters MRP3 and OSTα (organic solute transporter alpha) were significantly upregulated after BDL (Fig. 3D), suggesting that BAs may be more efficiently exported into the interstitium, from where they can reach the peritubular capillaries. In agreement with the RNA analysis, immunostaining of ASBT in the kidneys of mice after BDL did not show major changes compared to controls (Fig. 3E). Expression of ASBT occurred at the luminal side of TECs and was exclusively observed in AQP1-positive cells, a marker of proximal tubules (Fig. S8A). This is consistent with the functional analysis where fluorophore-coupled TCA showed a mosaic pattern with tubules that either do or do not reabsorb BAs (Fig. S8B). MALDI-MSI analysis of TCA supported the selective enrichment of TCA in ASBT-positive proximal TECs (Fig. S8C).

To study the translational relevance of the preserved ASBT expression in kidneys of cholestatic mice, a set of kidney biopsies from patients with early and advanced stages of CN, identified based on histopathological examination, was analyzed. Importantly, ASBT expression was preserved in patients with CN even at the late stages of the disease (Fig. 3F).

Evaluation of a systemic ASBT-specific inhibitor

To investigate the possible role of renal ASBT in the development of CN, we performed intervention studies with the novel compound AS0369 which has an IC_{50} of 1.31 nM for mouse ASBT and has >100-fold greater specificity for mouse ASBT *vs.* mouse NTCP (sodium-taurocholate co-transporting polypeptide) (Fig. 4A). After administration of 10 mg/kg AS0369 (per os) to wild-type mice, the mean C_{max} in blood was 222 nM (Fig. 4A; Fig. S9A) and the half-life was 2 h. Appreciable levels of AS0369 were also found in kidney tissue and in urine (Fig. 4A). To test the efficacy of AS0369 in the inhibition of renal ASBT *in vivo*, a pilot experiment was designed using female mice to allow for repeated urine collection by a urinary bladder catheter. Starting from day 7 post-BDL, the mice received various doses of AS0369 (15-120 mg/kg) orally twice per day for 5 days (Fig. 4B). Urine samples were collected daily, and blood samples were obtained 4-7 h post-dosing at day 5 for determination of plasma AS0369 and BA concentrations (Figs 4B and S9B). The lowest dose tested (15 mg/kg) increased urinary excretion of non-sulfated BAs (Fig. 4C). In contrast, little effect was observed on sulfated BAs, which are poor substrates of ASBT. Plasma concentrations of BAs were reduced with all tested doses of AS0369, but doses of 30-120 mg/kg were more effective than 15 mg/kg (Fig. 4D).

For a further pilot experiment with intravital imaging, a dose of 60 mg/kg AS0369 was selected; this dose evoked excessive increases in urinary BAs and was well tolerated. Interestingly, twice daily administration of AS0369 for 2 days, beginning on the day of BDL, strongly reduced the uptake of TCA into TECs (Fig. 4E), ameliorated oxidative stress in proximal TECs and tubular casts in distal tubules compared to vehicle-treated BDL mice (Fig. 4F). Therefore, a dose of 60 mg/kg was used for comprehensive efficacy studies.

Efficient prevention of CN by inhibition of renal ASBT

To evaluate the efficacy of AS0369 in the prevention of CN, a study design with female mice subjected to BDL and simultaneously treated with AS0369 (60 mg/kg, twice daily) or with vehicle for 6 weeks was performed. Sham-operated mice treated with vehicle served as controls (Fig. 5A). Treatment with AS0369 prevented mortality throughout the study period

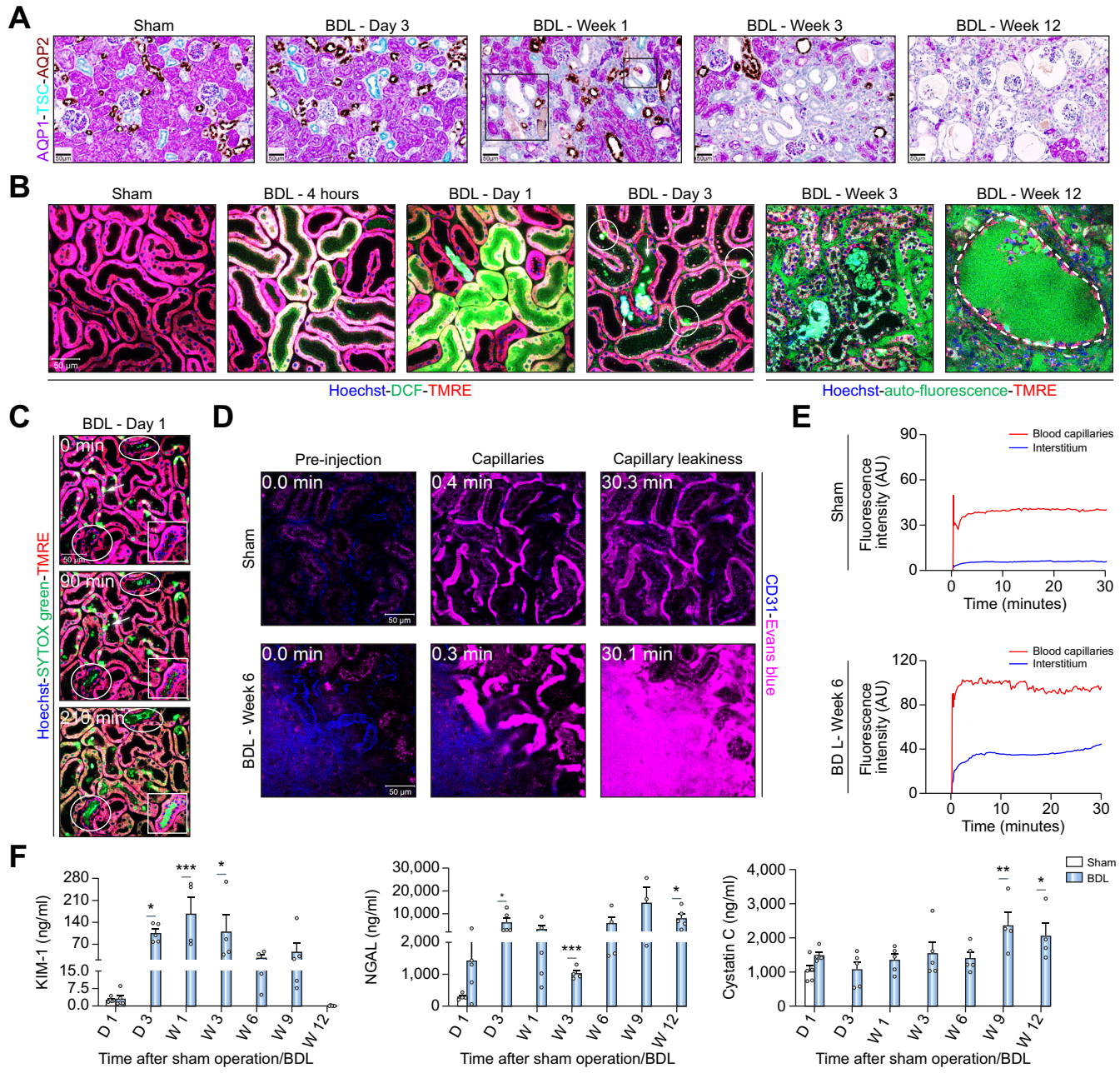

Fig. 2. Key events of CN. (A) Co-immunostaining of the proximal TEC marker AQP1, distal TEC marker TSC and the collecting duct marker AQP2 at various time periods after BDL. (B) Intravital imaging demonstrating oxidative stress of proximal TECs 4 h and 1 day after BDL based on the marker DCF. Dead proximal TECs (circles) and debris attached in distal tubules (arrows) on day 3 after BDL. Auto-fluorescence in (white arrows) and around peritubular capillaries at week 3 post BDL. Week 12 after BDL shows glomerular cysts (marked area). (C) Intravital imaging of dead proximal TECs based on the cytotoxicity marker SYTOX Green (arrowhead) at day 1 after BDL and formation of casts in a collecting duct (square) and distal tubules (circles) (Video S3A). (D) Leakiness of peritubular capillaries 6 weeks after BDL. Intravital imaging was performed after tail vein injection of Evans blue (magenta). Peritubular capillaries are visualized by anti-CD31 antibody (blue); scale bars: 50 μm. (E) Quantification of Evans blue signal in the peritubular capillaries and in the interstitium corresponding to Video S4. (F) Time course of kidney injury biomarkers in urine; data are presented as mean ± SEM; n = 5 mice per group. *p <0.05; **p <0.01; ***p <0.001 compared to the corresponding sham controls; Tukey's multiple comparisons test. The data are from male mice. BDL, bile duct ligation; D, day; DCF, dichlorofluorescein; TKIM1, kidney injury molecule; MRE, tetramethylrhodamine ethyl ester; NGAL, neutrophil gelatinase-associated lipocalin; W, week. (This figure appears in color on the web.)

compared to ~50% mortality in the vehicle-treated BDL group (Fig. 5B). In addition, BDL-induced body weight loss was prevented by treatment with AS0369 (Fig. 5C). The apparent body weight recovery in the BDL vehicle group by 6 weeks may be due in part to a dramatically increased gallbladder volume (Figs 5D,E and S10A). The BDL-associated increase in gallbladder volume was reduced by AS0369 (Fig. 5E). Furthermore, kidneys with a normal reddish-brown gross morphology were observed in the AS0369-treated BDL mice compared to kidneys with a greenish discoloration in the BDL vehicle group (Fig. 5D). The kidney-to-body weight ratio was not significantly altered in all groups, but the liver-to-body weight ratio showed a significant increase in the BDL vehicle group compared to the sham controls, which was ameliorated by AS0369 (Fig. S10B,C).

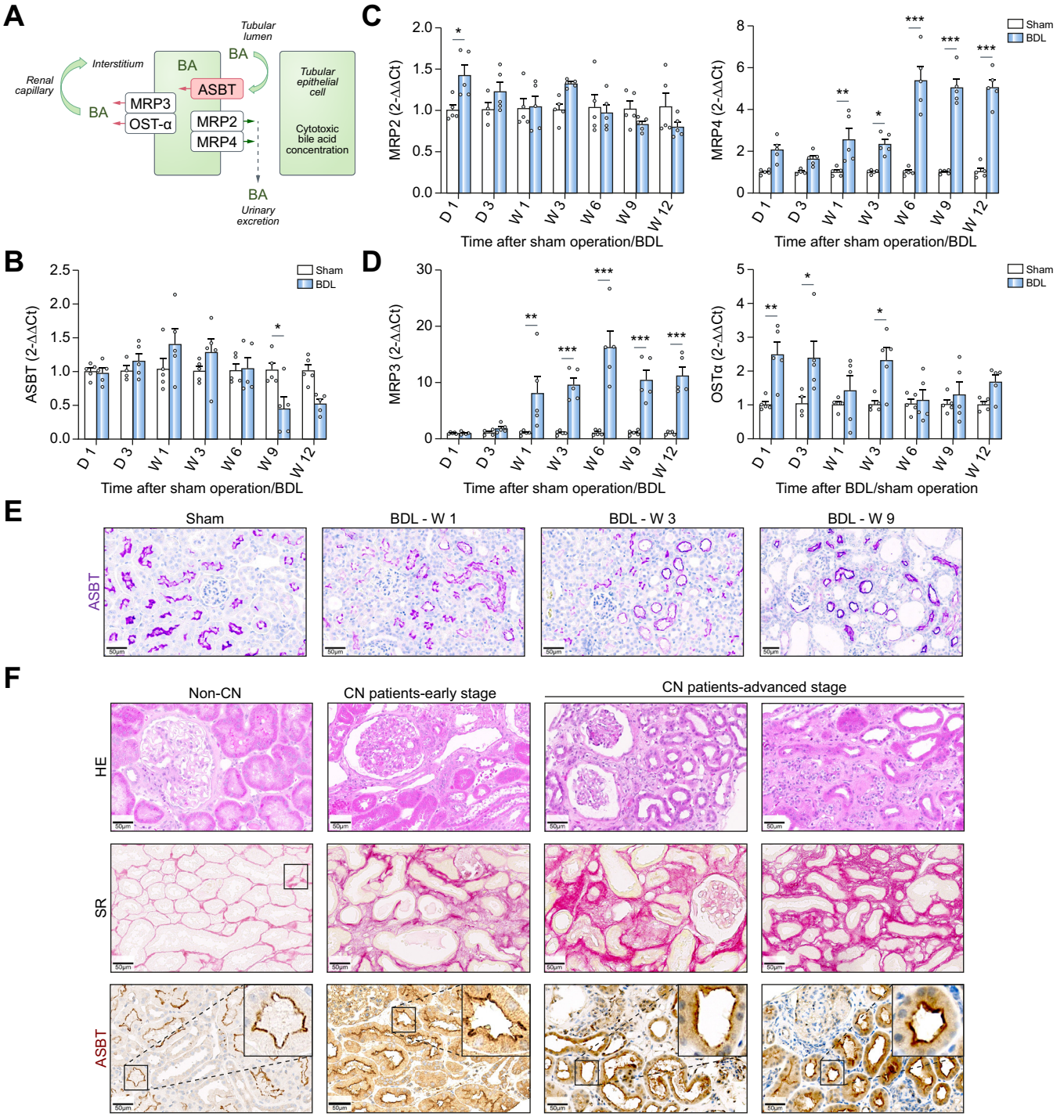

Fig. 3. Preserved ASBT expression in renal tissue of mice and patients with CN. (A) Schedule of BA transport in TECs. (B-D) RNA levels of BA transporters in renal tissue of mice at various periods after BDL compared to sham-operated mice; data are presented as mean ± SEM; n = 5 mice per group; *p <0.05; **p <0.01; ***p <0.001 compared to the corresponding controls; Tukey's multiple comparisons test. (E) Immunostaining of ASBT in renal tissue of mice after BDL. The data are from male mice. (F) ASBT expression in renal biopsies of patients with CN at early and advanced stages. Fibrosis was visualized by Sirius red (SR). Scale bars: 50 μm. ASBT, apical sodium-dependent bile acid transporter; CN, cholemic nephropathy; HE, haematoxylin and eosin; Mrp2/3/4, multidrug resistance-associated protein 2/3/4; Ostα, organic solute transporter alpha; SR, sirius red. (This figure appears in color on the web.)

Next, the effect of systemic ASBT inhibition with AS0369 on BA concentrations in relevant compartments was investigated. Urinary and renal tissue BA concentrations in the sham controls were very low, while they were elevated in response to BDL (Fig. 5F). Nonetheless, BA concentrations in urine were massively increased in the AS0369-treated *vs.* vehicle-treated BDL mice and were strongly reduced in liver and kidney tissue and in blood, whereas BA concentrations in bile were slightly increased (Fig. 5F). In agreement, MALDI-MSI analysis of TCA in liver and kidney tissues showed a strongly reduced signal in the

A

ASBT inhibitor (AS0369)

IC_{50} (nM)		PPB (%)	PK data after oral administration of 10 mg/kg					
ASBT	NTCP	99.6	Tmax (h)	Cmax (nM)	AUC last (h*nM)	$T_{1/2}$ (h)	Kidney concentration (µmol/g)	Urine concentration (nM)
1.31	178		2	222	837	2	0.4	1.05

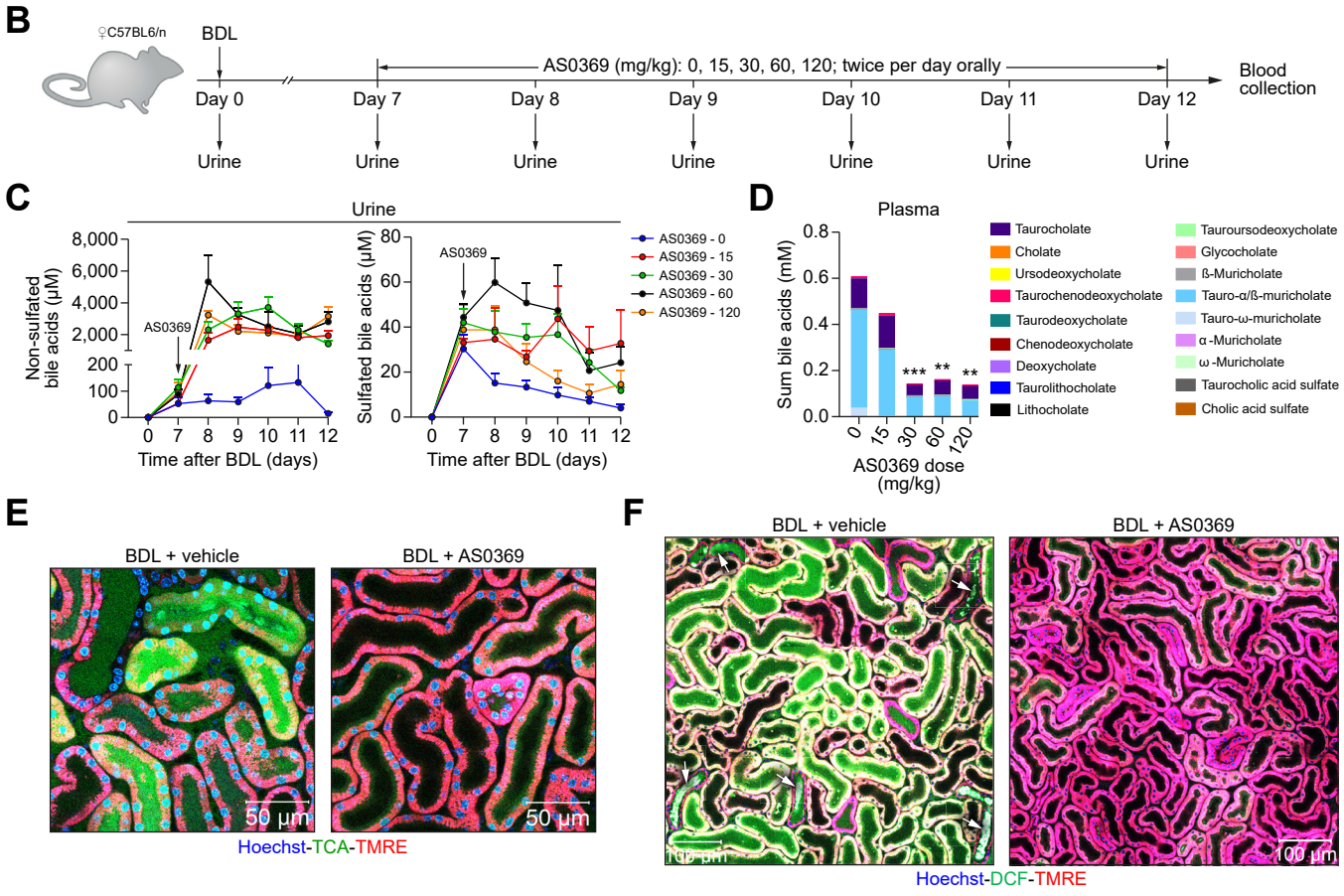

Fig. 4. Development of a systemic ASBT-specific inhibitor. (A) Inhibitory concentrations and pharmacokinetic data for AS0369. (B) Experimental schedule. (C, D) Concentrations of non-sulfated and sulfated BAs in urine and plasma after ASBT inhibition; data are presented as mean ± SEM; n = 3-6 mice per group; $^{**}p$ <0.01; $^{***}p$ <0.001 compared to the controls (0); Tukey's multiple comparisons test. (E) ASBT inhibition reduces TCA uptake into TECs. Intravital imaging was performed 3 days after BDL and AS0369 treatment (60 mg/kg, twice per day). Imaging was performed approximately 2 h after administration of the last AS0369 dose; scale bars: 50 µm. (F) Overview of renal tissue in mice on day 2 after BDL showing reduced oxidative stress and tubule casts after AS0369 treatment compared to vehicle treated mice; scale bars: 100 µm. The data in panels (E) and (F) are from male mice. ASBT, apical sodium-dependent bile acid transporter; BDL, bile duct ligation; DCF, dichlorofluorescein; NTCP, sodium-taurocholate co-transporting polypeptide; PPB, plasma protein binding; PK, pharmacokinetic; TCA, taurocholic acid; TMRE, tetramethylrhodamine ethyl ester. (This figure appears in color on the web.)

AS0369-treated mice compared to the BDL vehicle-treated group (Fig. 5G, H; Fig. S11). Treatment with AS0369 significantly reduced total serum bilirubin, alkaline phosphatase, and blood urea nitrogen, but not the liver damage biomarkers alanine and aspartate aminotransferase (Fig. 5I). AS0369 particularly reduced the TEC damage biomarker NGAL in urine (Fig. 5J). To study the effect of AS0369 at the tissue level, histological analysis of the kidney was performed. A strong reduction in leukocyte infiltration, fibrosis, tubule damage, cast formation, and endothelial cell damage was observed in the AS0369-treated BDL mice compared to vehicle-treated BDL mice (Figs 6A,B, S12 and 13A). In agreement, expression of early growth response protein 1, which plays a critical role in kidney fibrogenesis, was upregulated in kidney tissue after BDL and reduced to control levels by AS0369 (Fig. 6C). Furthermore, vascular leakage of Evans blue into the interstitium of kidney tissue after BDL was almost completely prevented by AS0369 (Figs 6D,G and S13B; Videos S5A-C). Sirius red staining of the liver showed periportal and perisinusoidal fibrosis in the vehicle treated BDL mice (Fig. S14). Treatment with AS0369 reduced the perisinusoidal fibrosis, and ameliorated canalicular dilatation (Fig. S14).

Next, the influence of ASBT inhibition on BA carrier expression in the liver and kidney and *Cyp7a1* expression in the liver was analyzed. AS0369 treatment did not significantly alter expression of the BA carriers in the liver compared to the BDL vehicle group, except that the BDL-induced upregulation of MRP4 was ameliorated in response to AS0369 (Fig. S15A). However, *Cyp7a1* expression was upregulated after AS0369 treatment (Fig. S15A). In kidney tissue, AS0369 treatment

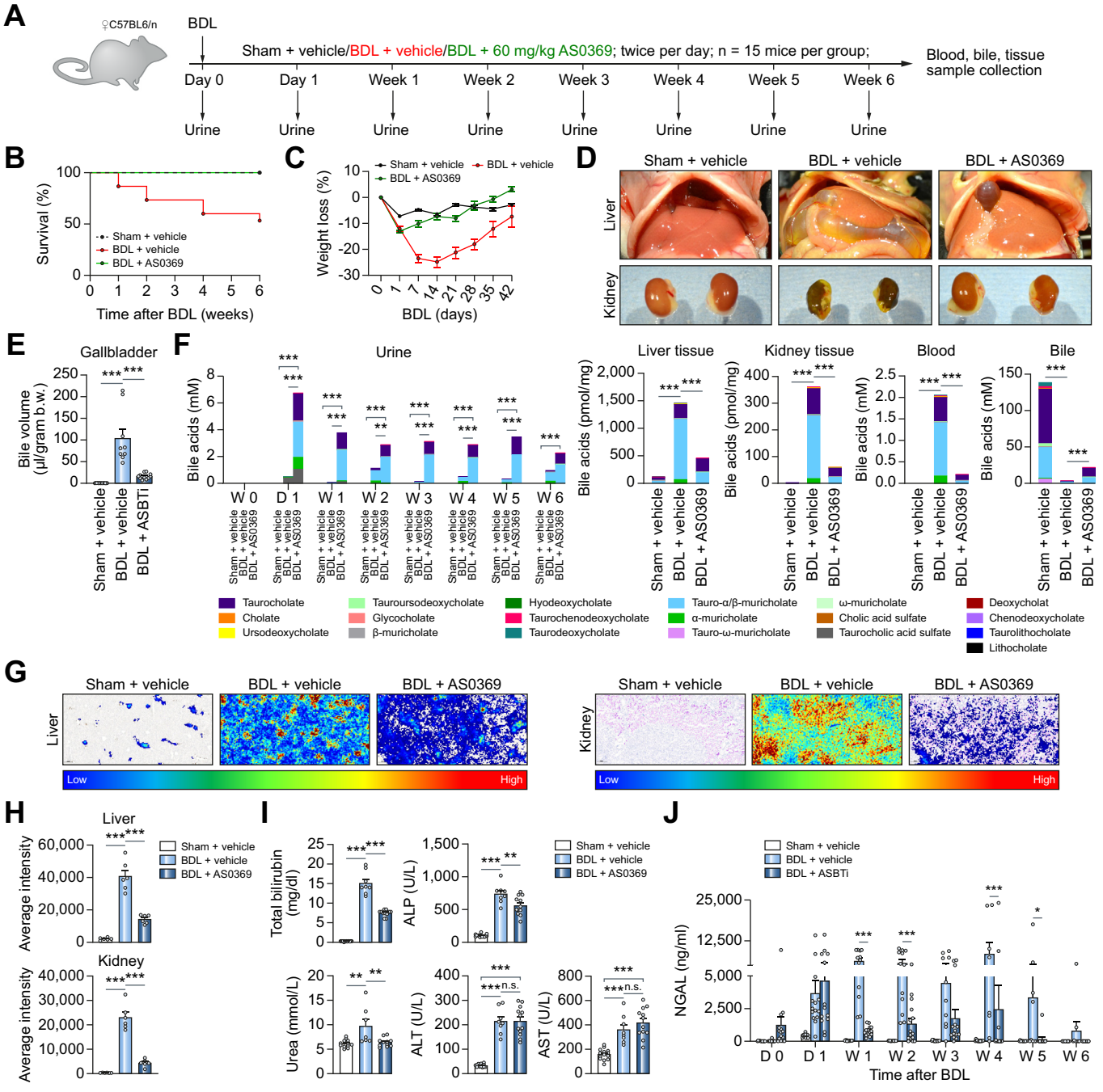

Fig. 5. Efficient prevention of CN by inhibition of renal ASBT. (A) Experimental schedule. (B, C) Survival analysis and body weight changes. (D) Gross pathology of mouse livers and kidneys. (E) Gallbladder bile volume. (F) BA concentrations in urine, liver, and kidney tissues, blood, and bile. ***p <0.001, Tukey's multiple comparisons test. (G, H) MALDI-MSI analysis of taurocholic acid in liver and kidney tissues, and corresponding quantifications. (I, J) Blood (total bilirubin, alkaline phosphatase, urea, ALT, AST) and urine (NGAL) biomarkers of liver and kidney damage. *p <0.05, ***p <0.001, Tukey's multiple comparisons test. Data are presented as mean ± SEM. The data are from female mice. ALP, alkaline phosphatase; ALT, alanine transaminase; AST, aspartate transaminase; BDL, bile duct ligation; NGAL, neutrophil gelatinase-associated lipocalin. (This figure appears in color on the web.)

prevented the BDL-induced dysregulation of BA carrier expression except for MRP4 (Fig. S15B).

Since the main intervention study was performed in female mice, we repeated the intervention experiment using male mice, with the difference that urine was only collected at the end of the 6-week treatment. The results confirmed the remarkable protection against development of CN conferred by AS0369 and showed that this effect is not sex specific (Figs S16 and S17).

RNA-sequencing reveals large effect size of ASBT inhibition

To perform an unbiased evaluation of the effect of ASBT inhibition at the transcriptional level, kidney and liver tissues were analyzed by RNA-sequencing. The kidney samples from BDL mice treated with AS0369 clustered closer to controls than to vehicle-treated BDL mice in a principal component analysis (Fig. 7A), indicating a sizable effect of AS0369 treatment in the kidney, which was also reflected by many significantly up and

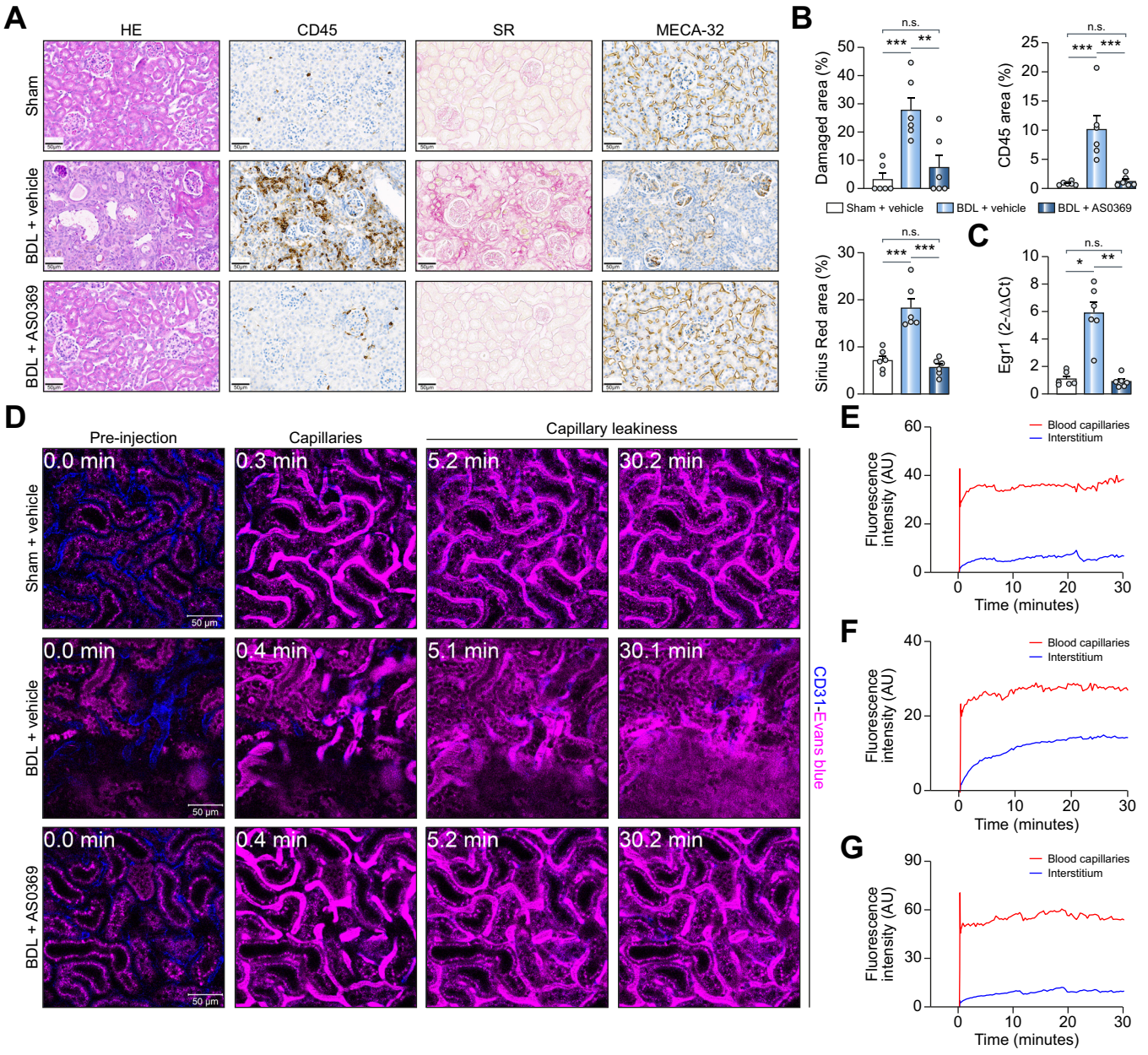

Fig. 6. Prevention of peritubular capillary leakiness by ASBT inhibition. (A,B) Histopathology and immunostaining of leukocyte (CD45), and endothelial cells (MECA-32) in the three treatment groups illustrated in Fig 5A, and corresponding quantifications; scale bars: 50 µm. (C) RNA levels of *Egr1* in renal tissue; *p <0.05, **p <0.01, ***p <0.001; Tukey's multiple comparisons test. Data are presented as mean ± SEM. (D-G) Intravital imaging after tail vein injection of Evans blue (magenta) and the corresponding quantifications in the peritubular capillaries and the interstitium (Videos S5A-C). The peritubular capillaries are visualized by anti-CD31 antibody (blue); scale bars: 50 µm. The data are from female mice. BDL, dile duct ligation; CD45, cluster of differentiation 45, Egr1, early growth response protein-1; HE, haematoxylin and eosin; MECA-32, mouse endothelial cell antigen-32; SR, sirius red. (This figure appears in color on the web.)

downregulated genes (Fig. 7B). To further investigate this effect, genes were plotted by their log2-fold-changes over controls for vehicle-treated (x-axis) and AS0369-treated (y-axis) BDL mice (Fig. 7C), delineating five gene groups: genes in group 1a and 2a were upregulated by BDL and downregulated by AS0369, either completely to control levels (1a) or partially (2a). Conversely, genes in 1b and 2b were downregulated in response to BDL, which was either completely (1b) or partially (2b) prevented by AS0369. Only relatively few genes were induced by AS0369 treatment but not affected by BDL, representing AS0369-specific response genes (3a). Overrepresentation analysis demonstrated an enrichment in inflammation-associated gene ontology groups for genes upregulated due to BDL, while the downregulated genes were associated with metabolic processes (Fig. 7D). Correspondingly, genes upregulated by BDL and downregulated to control levels by AS0369 (1a) were also inflammation-associated, and genes downregulated by BDL and increased to control levels by AS0369 (1b) also represented metabolic gene ontology groups (Fig. 7E). The most downregulated gene upon ASBT inhibition in group 1a was the extracellular matrix protein COL10A1, and the most upregulated gene in group 1b was histidine decarboxylase, which catalyzes the synthesis of histamine (Fig. 7F). Qualitatively similar consequences of ASBT inhibition were observed in the livers of the

same mice, but the effect was smaller (Fig. 7G-L). Nevertheless, the overlaps of altered genes in the liver and kidney were higher than randomly expected (Fig. S18). Altogether, the RNA-sequencing analysis demonstrated that AS0369 treatment ameliorated BDL-induced gene expression in the kidney, while the effects in the liver were smaller.

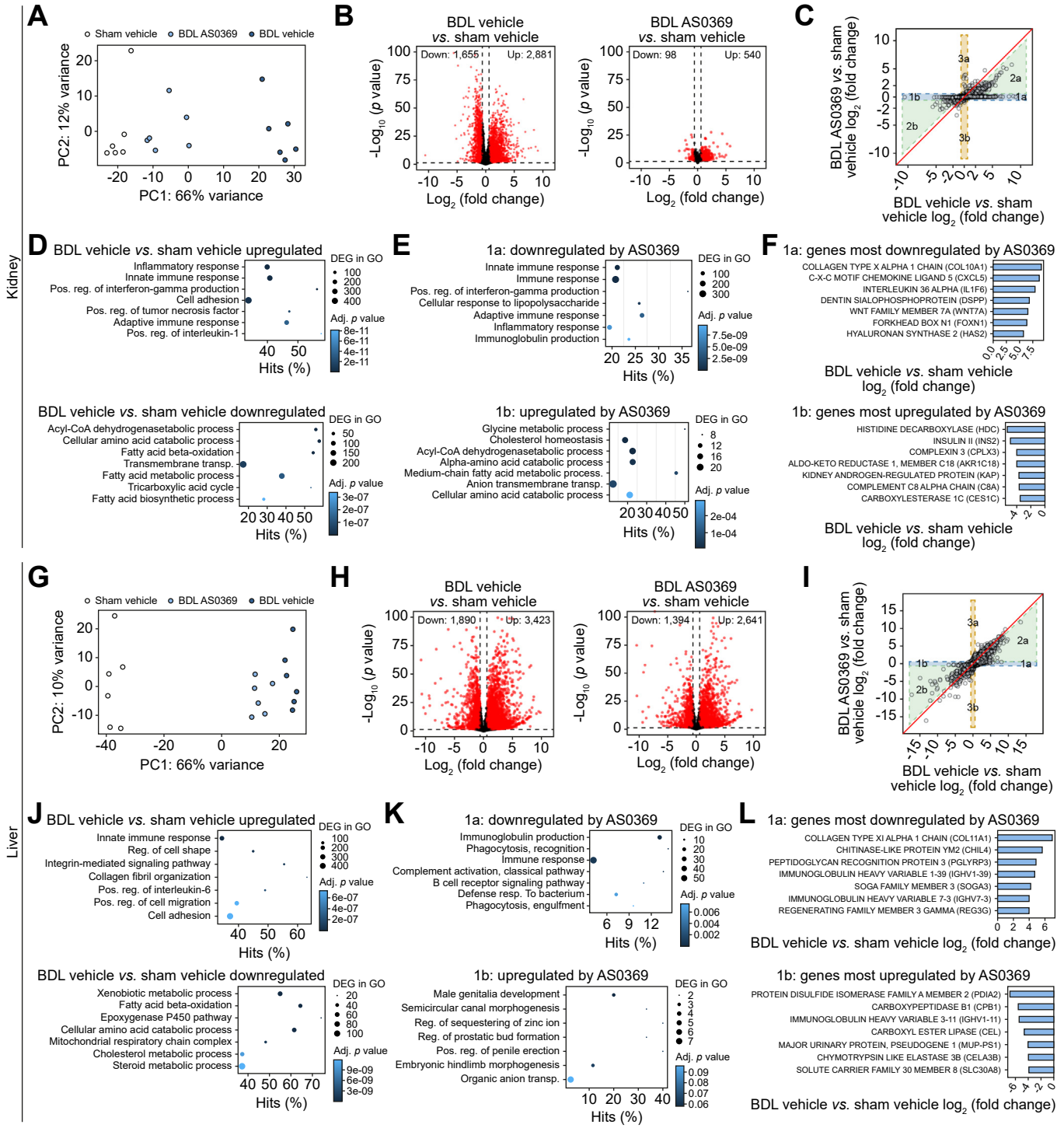

Fig. 7. RNA-seq analysis of BDL mice confirms the protective effect of ASBT inhibition in the kidney and liver. (A) PCA plots of sham vehicle mice, BDL mice treated with the vehicle, and BDL mice treated with AS0369. Each dot represents an individual mouse. (B) Volcano plots illustrating differential genes between vehicle-treated (left panel) and AS0369-treated (right panel) mice with BDL and controls (sham vehicle). (C) DiPa plots illustrating the response to AS0369. Each dot represents an individual gene. (D, E) Plots of overrepresented GO groups in the indicated differential gene sets. The size of the dots represents the number of genes in the individual GO groups and the color code the adjusted (adj) *p* value. (F) Genes most influenced by AS0369 in groups 1a and 1b of the DiPa plot. (G-L) correspond to A-F but were performed with liver tissue. The data are from female mice. BDL, bile duct ligation; PCA, Principal component analysis. (This figure appears in color on the web.)

Translational relevance

Large differences in BA synthesis and composition are known between humans and mice. Therefore, we used the *Cyp2c70*$^{-/-}$ mice with humanized BA spectrum[19] that – like humans – have lower total BAs but higher concentrations of the more toxic BA chenodeoxycholic acid, and very low levels of hydrophilic muricholate BA (Fig. 8A-C). AS0369 also increased sum BA concentrations in the urine of the *Cyp2c70*$^{-/-}$ mice (Fig. 8A), including BAs that are formed by humans but not (or only at very low concentrations) by mice, such as taurochenodeoxycholic acid (Fig. 8B). Upon BDL, *Cyp2c70*$^{-/-}$ mice showed aggravated kidney injury compared to wild-type mice, as illustrated by higher levels of NGAL (Fig. 8C). *Cyp2c70*$^{-/-}$ mice could not be analyzed for periods longer than 24 h after BDL, because of their poor health status that was much worse compared to that of wild-type mice. It took about 1 week for AS0369 to reduce NGAL in WT mice after BDL (Fig. 5J). However, in *Cyp2c70*$^{-/-}$ mice, a significant reduction in NGAL was already seen at day 1 in male mice, with a trend in female mice (Fig. 8C). Thus, AS0369 also enhances urinary excretion of a humanized and more hydrophobic spectrum of BAs and ameliorated BDL-induced kidney injury.

To address the translational relevance of the findings in mice, we studied patients with acute and/or chronic liver disease with serum bilirubin >6 mg/dl (n = 67) and healthy volunteers (n = 36) and focused on the relationship between sum BA and bilirubin concentrations in serum and the proximal TEC damage marker KIM-1 (patient characteristics: Table S1B). Besides liver enzymes, bilirubin, and BA, blood urea nitrogen, cystatin C, NGAL, and KIM-1 were significantly increased in patients compared to healthy volunteers (Fig. 8D). Among patients with acute and/or chronic liver disease, sum BA concentrations correlated positively with bilirubin levels (Fig. 8E) and both bilirubin and BA correlated positively with KIM-1 (Fig. 8F,G). In a multiple linear regression model after backward selection, only sum BA was kept as an explanatory variable for KIM-1, while bilirubin, C-reactive protein (a marker of systemic inflammation, which may contribute to kidney injury), and ursodeoxycholic acid therapy were excluded (Fig. 8H).

Discussion

The mechanisms of CN pathogenesis remain poorly understood, and no specific treatments are available.[3,6] Therefore, we studied the pathomechanisms of BDL-induced CN in mice by intravital imaging and observed five subsequent events: i. BA increase in blood and enrichment in proximal TECs (almost immediately after BDL); ii. oxidative stress in proximal TECs (4 h onwards); iii. death of proximal TECs with release of debris into the tubular lumen, which travels downstream and forms casts in the distal tubules and collecting ducts, followed by dilatation of tubules (day 1-3 onwards); iv. peritubular capillary damage and leakiness (week 3 onwards); and v. glomerular cysts (week 6 onwards).

ASBT is known to transport BAs from the tubular lumen into TECs. Therefore, to study a possible causal relationship between BA enrichment and oxidative stress, as well as cell death of proximal TECs, we utilized the systemically bioavailable specific ASBT inhibitor, AS0369, which blocked the uptake of BAs into TECs almost completely. A remarkable finding was the large effect size of AS0369, and the renal protective effects associated with decreasing kidney BA levels. All CN hallmarks (event i-v) were almost completely absent with twice daily AS0369 administration over a 6-week period after BDL.

Targeting renal ASBT not only provides renal protective effects but also serves as a means of lowering overall BA load in the body by increasing urinary excretion. Indeed, plasma BA concentrations decreased strongly in response to AS0369. Importantly, the elevated urine BA levels induced by AS0369 also offer a non-invasive biomarker of renal ASBT target engagement which may have translational value. Plasma levels of AS0369 dosed at 60 mg/kg were approximately 200 nmol/L 4-7 h after administration. Since AS0369 is tightly protein bound (>99%), free plasma levels were approximately 1-2 nmol/L which equates to the ASBT IC_{50}, suggesting that the observed efficacy was not due to off-target interactions.

While TEC death occurred within the first days after BDL (event i-iii), compromised capillary endothelial cells were observed at week 3 onwards (event iv). This led to peritubular capillary leakage and is possibly explained by endothelial cell damage caused by an elevated flux of BAs from the tubule lumen into the interstitial space, although elevated circulating BAs could also contribute. Nonetheless, AS0369 treatment substantially improved renal peritubular capillary integrity.

The protective effect of AS0369 in the kidneys was also reflected in the genome-wide analyses, where AS0369 reduced the number of genes deregulated by BDL to a larger degree in the kidney than the liver. A plausible explanation for the stronger effect in the kidney is that TECs are specifically protected against BA overload by AS0369, since ASBT appears to be the sole mechanism for reabsorption of non-sulfated BAs from the tubule lumen. Conversely, hepatocytes continue to synthesize BAs and AS0369 does not affect hepatocellular sinusoidal BA uptake via NTCP and OATPs (organic anion transporting proteins). As such, the liver BA content remains elevated above normal levels in this model of complete biliary tract obstruction. These findings generally agree with a recently published study, where whole body ASBT knockout mice showed decreased liver damage 5 days after BDL.[20] In addition, administration of an intestine-restricted ASBT inhibitor in combination with the farnesoid X receptor agonist obeticholic acid lowered the BA pool, and ameliorated liver injury 2-days post-BDL.[20]

Systemic ASBT inhibition has multiple favorable consequences in advanced liver diseases. Blocking renal ASBT specifically protects a subset of TECs that are vulnerable to BA toxicity and prevents CN (so-called organ-protection). Moreover, increased urinary elimination of non-sulfated BAs, which lowers the overall BA pool, is favorable for all cell types compromised by exposure to high levels of circulating BAs. Importantly, in *Cyp2c70*$^{-/-}$ mice, that have a humanized BA composition,[19] we observed that AS0369 also enhanced urinary excretion of the more toxic hydrophobic BAs, such as taurochenodeoxycholic acid, and ameliorated kidney injury after BDL, indicating a possible human relevance.

An initial key event of CN in mice is the accumulation of BAs in proximal TECs, cell death and the release of KIM-1 from this cell type. Since KIM-1 is also considered a marker of proximal TEC injury in humans,[2] we analyzed KIM-1 in serum of patients with acute and/or chronic liver disease and hyperbilirubinemia. The sum BA concentration was the key explanatory variable in

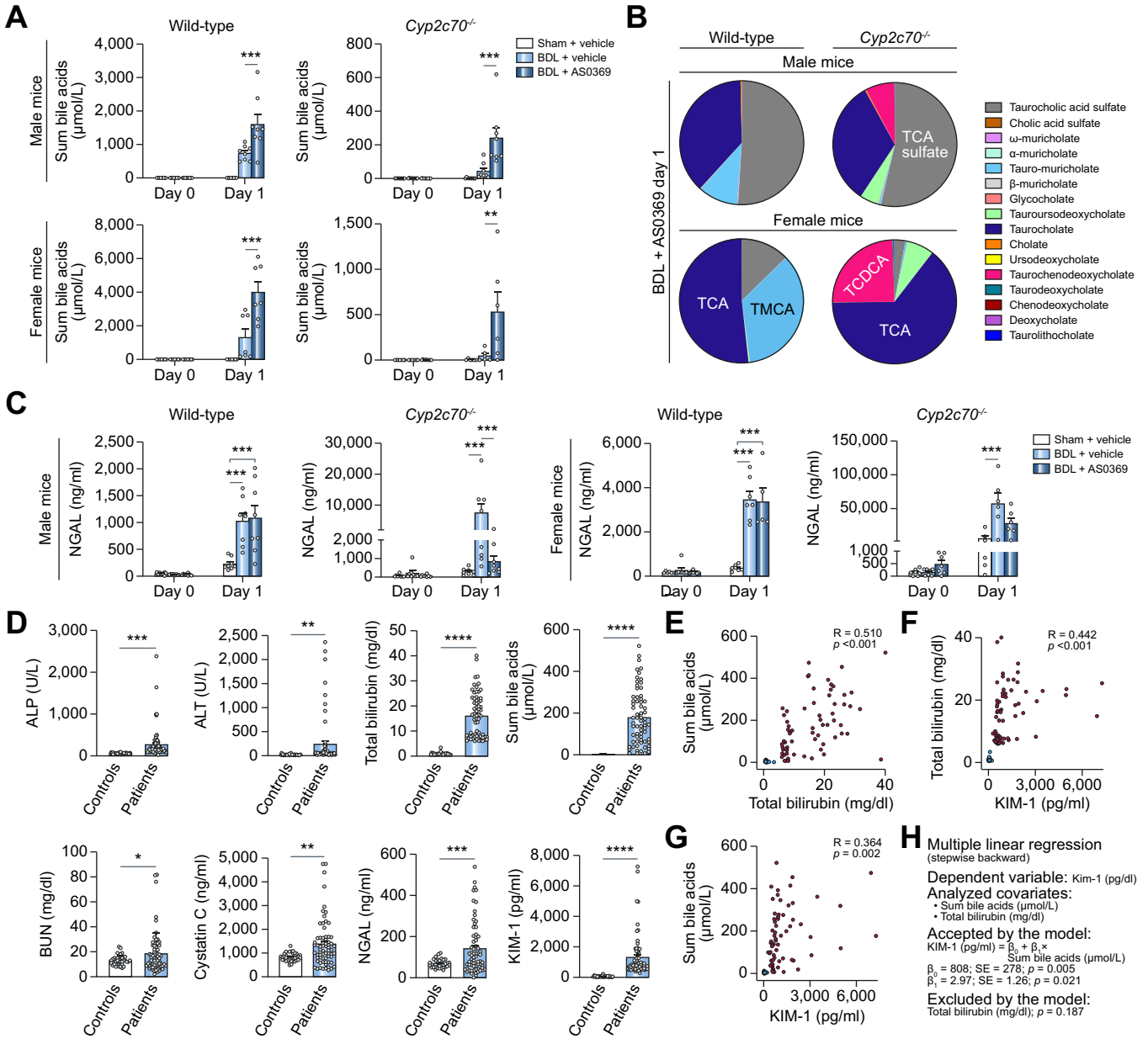

Fig. 8. Translational relevance. (A-C) Analysis of mice with humanized BA spectrum; *Cyp2c70*$^{-/-}$. (A) Urine BAs in mice after sham surgery, BDL and vehicle administration, and BDL plus 60 mg/kg AS0369 twice, on day 1. (B) Individual BAs in wild-type and *Cyp2c70*$^{-/-}$ mice. (C) Urine NGAL in male and female wild-type and *Cyp2c70*$^{-/-}$ mice. $^{**}p$ <0.01, $^{***}p$ <0.001; Tukey's multiple comparisons test. (D-H) Analysis of patients with acute and/or chronic liver disease and hyperbilirubinemia. (D) Liver enzymes, bilirubin, BA and kidney injury markers in serum of patients and in healthy volunteers (controls). $^{*}p$ <0.05, $^{**}p$ <0.01, $^{***}p$ <0.001, $^{****}p$ <0.0001; Unpaired t-test. (E-G) Spearman's correlation of BA, bilirubin, and KIM-1 in serum of patients (red circles) and heathy volunteers (blue circles); R: correlation coefficient; P: Spearman's *p* value. (H) Multiple linear regression analysis with serum KIM-1 as a dependent variable. ALP, alkaline phosphatase; ALT, alanine transaminase; BDL, bile duct ligation; BUN, blood urea nitrogen; KIM1, kidney injury molecule; NGAL, neutrophil gelatinase-associated lipocalin. (This figure appears in color on the web.)

a multiple linear regression model with KIM-1 as the dependent variable, suggesting that BAs may play a pivotal role in human kidney injury in the context of liver dysfunction. The present human data does not exclude that bilirubin (and possibly additional cholephiles released from the liver) may be relevant, considering that patients were selected based on a cut-off of >6 mg bilirubin/dl. The latter was chosen as it denotes liver dysfunction in the context of decompensated cirrhosis[4] and an analysis of 1,372 patients included in the above-mentioned registry study found that profound elevations of BA are uncommon in patients with lower bilirubin values (data not shown). Notably, mean arterial pressure (as a marker of circulatory dysfunction) was not included in our models, as all bar two patients with mean arterial pressures of 64 mmHg had pressures ≥65 mmHg and C-reactive protein (as a marker of systemic inflammation) was less closely associated with proximal TEC injury than sum BA concentration.

At first glance, it may be surprising that the earliest key events of CN occur in proximal tubules in the present mouse study, as casts are observed in distal tubules in human biopsies.[2] The herein described mechanism resolves this discrepancy, since debris from dead proximal TECs travels

downstream in the tubule lumen to induce cast formation in distal tubules and collecting ducts; compartments with a high luminal osmolarity. In biopsies only the latter cast formation but not the initial death events in proximal TECs can be detected. A further translationally relevant component of the herein described mechanisms is that ASBT expression is preserved in patients with CN at the luminal side of proximal TECs.

In conclusion, a mouse model of CN identified BA enrichment in TECs as a critical pathomechanism. Blocking renal ASBT-mediated BA reabsorption prevented CN development and systemically decreased BA concentrations. Taken together, systemically available ASBT inhibitors reaching the kidney may exert reno-protective effects in conditions of kidney injury secondary to liver disease.

Affiliations

[1]Department of Toxicology, Leibniz Research Centre for Working Environment and Human Factors, Technical University Dortmund, Ardeystr. 67, 44139 Dortmund, Germany; [2]Department of Forensic Medicine and Toxicology, Faculty of Veterinary Medicine, South Valley University, 83523 Qena, Egypt; [3]Albireo Pharma, Inc., Boston, MA 02109, USA; [4]Dr. Margarete Fischer-Bosch Institute of Clinical Pharmacology and University of Tübingen, Auerbachstr. 112, 70376 Stuttgart, Germany; [5]Department of Statistics, TU Dortmund University, 44227 Dortmund, Germany; [6]Institute of Computer Science & Saxonian Incubator for Clinical Research (SIKT), University of Leipzig, Haertelstraße 16-18, 04107 Leipzig, Germany; [7]Department of Gastroenterology, Hepatology and Infectious Diseases, University Hospital Duesseldorf, Medical Faculty at Heinrich-Heine-University, 40225 Dusseldorf, Germany; [8]Histology Department, Faculty of Medicine, South Valley University, 83523 Qena, Egypt; [9]Department of Pharmacology, Faculty of Veterinary Medicine, Sohag University, 82524 Sohag, Egypt; [10]Department of Pharmacology, Faculty of Veterinary Medicine, South Valley University, 83523 Qena, Egypt; [11]Department of Biomedical Sciences, An-Najah National University, P.O. Box 7 Nablus, Palestine; [12]Department of Pharmacy, An-Najah National University, P.O. Box 7 Nablus, Palestine; [13]MRI Unit, Leibniz Research Centre for Working Environment and Human Factors, Department of Psychology and Neurosciences, Technical University Dortmund, 44139 Dortmund, Germany; [14]Department of Molecular and Clinical Medicine/Wallenberg Laboratory, Sahlgrenska Academy, University of Gothenburg, 41345 Gothenburg, Sweden; [15]University Clinic for Visceral Surgery and Medicine, Inselspital University Hospital, University of Bern, 3010 Bern, Switzerland; [16]Departments of Clinical Pharmacology, and of Biochemistry and Pharmacy, University Tuebingen, 72076 Tuebingen, Germany; [17]Cluster of Excellence iFIT (EXC2180), Image-Guided and Functionally Instructed Tumor Therapies, University of Tuebingen, 69120 Tuebingen, Germany; [18]Institute of Pathology and Department of Nephrology, University Hospital RWTH Aachen, Pauwelsstr. 30, 52074 Aachen, Germany; [19]Department of Nephropathology, Friedrich-Alexander-University Erlangen-Nuremberg, 91054 Erlangen, Germany; [20]Institute of Pathology, Nephropathology Unit, Hannover Medical School, 30625 Hannover, Germany; [21]Department of Pediatrics, Division of Gastroenterology, Hepatology, and Nutrition, Emory University, Atlanta, GA 30322, United States; [22] Division of Gastroenterology and Hepatology, Department of Internal Medicine III, Medical University of Vienna, 1090 Vienna, Austria; [23]Vienna Hepatic Hemodynamic Lab, Division of Gastroenterology and Hepatology, Department of Internal Medicine III, Medical University of Vienna, Vienna, Austria; [24]Hans Popper Laboratory of Molecular Hepatology, Vienna Hepatic Hemodynamic Lab, Division of Gastroenterology and Hepatology, Department of Internal Medicine III, Medical University of Vienna, Vienna, Austria

Abbreviations

AKI, acute kidney injury; AQP, aquaporin; ASBT, apical sodium-dependent bile acid transporter; BAs, bile acids; BDL, bile duct ligation; CN, cholemic nephropathy; KIM-1, kidney injury molecule 1; MALDI-MSI: matrix assisted laser desorption/ionization mass spectrometry imaging; MRP, multidrug resistance-associated protein; NGAL, neutrophil gelatinase-associated lipocalin; TCA, taurocholic acid; TECs, tubular epithelial cells.

Financial support

A.G. was funded by the German Research Foundation (DFG; Project IDs 517010379& 457840828). PB was supported by the DFG (Project IDs 322900939, 454024652, 432698239 & 445703531), European Research Council (ERC Consolidator Grant No 101001791), and the Federal Ministry of Education and Research (BMBF, STOP-FSGS-01GM2202C). JR, JD, CD, FK were funded by the Research Training Group "Biostatistical Methods for High-Dimensional Data in Toxicology" (RTG 2624, Project P2) funded by the DFG (Project Number 427806116). PAD was supported by NIH DK047987. MS was supported by the DFG im Rahmen der Exzellenzstrategie des Bundes und der Länder-EXC 2180-390900677. UH and MS were in parts supported by the Robert Bosch Stiftung Stuttgart, Germany.

Conflict of interest

AG and JGH declare consulting activities for Albireo Pharma. ES and EL are employees of Albireo Pharma. HUM declares consulting or advisory board activities for Albireo Pharma, Calliditas, Intercept, Mirum and Zealand and lecture fees by Albireo, Intercept and Bayer. SJK declares consulting activities for Albireo Pharma, Hemoshear, Intercept Pharma, and Mirum Pharma; PAD has received research grants from Albireo Pharma. B.S. received travel support from AbbVie and Gilead. TR received grant support from Abbvie, Boehringer Ingelheim, Gilead, Intercept/Advanz Pharma, MSD, Myr Pharmaceuticals, Philips Healthcare, Pliant, Siemens and W. L. Gore & Associates; speaking honoraria from Abbvie, Gilead, Intercept/Advanz Pharma, Roche, MSD, W. L. Gore & Associates; consulting/advisory board fee from Abbvie, Astra Zeneca, Bayer, Boehringer Ingelheim, Gilead, Intercept/Advanz Pharma, MSD, Resolution Therapeutics, Siemens; and travel support from Abbvie, Boehringer Ingelheim, Dr. Falk Pharma, Gilead and Roche. M.M. served as a speaker and/or consultant and/or advisory board member for AbbVie, Collective Acumen, Echosens, Gilead, Ipsen, Takeda, and W. L. Gore & Associates and received travel support from AbbVie and Gilead. MT received speaker fees from BMS, Falk Foundation, Gilead, Intercept, Jannsen, Madrigal, and MSD; he advised for Abbvie, Albireo Pharma, BiomX, Boehringer Ingelheim, Falk Pharma GmbH, Genfit, Gilead, Hightide, Intercept, Janssen, MSD, Novartis, Phenex, Pliant, Regulus, Siemens and Shire. He further received travel grants from Abbvie, Falk, Gilead, Intercept and Jannsen and research grants from Albireo Pharma, Alnylam, Cymabay, Falk, Gilead, Intercept, MSD, Takeda and UltraGenyx. He is also co-inventor of patents on the medical use of norUDCA filed by the Medical Universities of Graz and Vienna. MS received travel expenses and research support from Agena Bioscience, CED Service GmbH, and ALL Akademie. MS was involved in clinical trials by Green Cross WellBeing Co.Ltd., Gilead Sciences Inc., CORAT Therapeutics GmbH, Agena Bioscience, and HepaRegenix GmbH.

Please refer to the accompanying ICMJE disclosure forms for further details.

Authors' contributions

AG and JGH: study concept and design, data acquisition, analysis and interpretation of data, manuscript writing, funding, study supervision; DG, MM, RH, ZH, LB, BBT, JR, MV, AS, TA, NA, SAFM, WM, AH, WA, NV, CV, RM, CC, MV, EG, PN, SJK: contributed to study concept and design, data acquisition, manuscript writing, analysis and interpretation of data; ES, PÅ, JM, EL: synthetized AS0369, contributed to study concept and design, data acquisition, manuscript writing, analysis and interpretation of data, funding; UH, MS: bile acid analysis, contributed to manuscript writing, critical revision of the manuscript; JD, CD, FK, JR: bioinformatics analysis, contributed to manuscript writing, critical revision of the manuscript; AF, SH: image analysis, contributed to manuscript writing, critical revision of the manuscript; NK, MA, AS: synthetized fluorescein-coupled TCA, contributed to manuscript writing, critical revision of the manuscript; KE: RNA-sequencing, contributed to bioinformatics analysis, study concept and design, data acquisition, analysis and interpretation of data, critical revision of the manuscript; KA, JS, JHB, PB, BS, TR, MM: clinical data; contributed to study concept and design, analysis and interpretation of data, critical revision of the manuscript; MT, HUM, PAD, GS, TL: contributed to study concept and design, analysis and interpretation of data, critical revision of the manuscript.

Data availability statement

All data presented in this manuscript will be made available to other researchers upon request.

Acknowledgment

We would like to acknowledge Ingemar Starke, Per-Göran Gillberg (Albireo Pharma Inc, Boston, MA, USA) and Santosh Kulkarni, Runa Pal, Atul Tiwari,

Shivendra Singh, Ramesh Kangarajan, Ashwani Gaur (Syngene International, Bangalore, India) for their contributions to the development of AS0369.

Supplementary data

Supplementary data to this article can be found online at https://doi.org/10.1016/j.jhep.2023.10.035.

References

Author names in bold designate shared co-first authorship.

[1] EASL., EASL. Clinical Practice Guidelines for the management of patients with decompensated cirrhosis. J Hepatol 2018;69:406–460.
[2] Krones E, Pollheimer MJ, Rosenkranz AR, et al. Cholemic nephropathy - historical notes and novel perspectives. Biochim Biophys Acta Mol Basis Dis 2018;1864:1356–1366.
[3] Somagutta MR, Jain MS, Pormento MKL, et al. Bile cast nephropathy: a comprehensive review. Cureus 2022;14:e23606.
[4] Mandorfer M, Aigner E, Cejna M, et al. Austrian consensus on the diagnosis and management of portal hypertension in advanced chronic liver disease (Billroth IV). Wien Klin Wochenschr 2023;135:493–523.
[5] Simbrunner B, Trauner M, Reiberger T, et al. Recent advances in the understanding and management of hepatorenal syndrome. Fac Rev 2021;10:48.
[6] Fickert P, Rosenkranz AR. Cholemic nephropathy reloaded. Semin Liver Dis 2020;40:91–100.
[7] Mandorfer M, Hecking M. The renaissance of cholemic nephropathy: a likely underestimated cause of renal dysfunction in liver disease. Hepatology 2019;69:1858–1860.
[8] **Ariza X**, **Graupera I**, Coll M, et al. Neutrophil gelatinase-associated lipocalin is a biomarker of acute-on-chronic liver failure and prognosis in cirrhosis. J Hepatol 2016;65:57–65.
[9] Arroyo V, Moreau R, Jalan R, et al. Acute-on-chronic liver failure: a new syndrome that will re-classify cirrhosis. J Hepatol 2015;62:S131–S143.
[10] Nayak SL, Kumar M, Bihari C, et al. Bile cast nephropathy in patients with acute kidney injury due to hepatorenal syndrome: a postmortem kidney biopsy study. J Clin Transl Hepatol 2017;5:92–100.
[11] **Fickert P**, **Krones E**, Pollheimer MJ, et al. Bile acids trigger cholemic nephropathy in common bile-duct-ligated mice. Hepatology 2013;58:2056–2069.
[12] Krones E, Eller K, Pollheimer MJ, et al. NorUrsodeoxycholic acid ameliorates cholemic nephropathy in bile duct ligated mice. J Hepatol 2017;67:110–119.
[13] Allegretti AS, Belcher JM. Bile acids are important contributors to AKI associated with liver disease: CON. Kidney360 2022;3:21–24.
[14] Fickert P, Rosenkranz AR. Bile acids are important contributors to AKI associated with liver disease: pro. Kidney360 2022;3:17–20.
[15] Ghallab A, Hassan R, Hofmann U, et al. Interruption of bile acid uptake by hepatocytes after acetaminophen overdose ameliorates hepatotoxicity. J Hepatol 2022;77:71–83.
[16] Ghallab A, Hofmann U, Sezgin S, et al. Bile microinfarcts in cholestasis are initiated by rupture of the apical hepatocyte membrane and cause shunting of bile to sinusoidal blood. Hepatology 2019;69:666–683.
[17] Bábíčková J, Klinkhammer BM, Buhl EM, et al. Regardless of etiology, progressive renal disease causes ultrastructural and functional alterations of peritubular capillaries. Kidney Int 2017;91:70–85.
[18] Wilson FA, Burckhardt G, Murer H, et al. Sodium-coupled taurocholate transport in the proximal convolution of the rat kidney in vivo and in vitro. J Clin Invest 1981;67:1141–1150.
[19] Truong JK, Bennett AL, Klindt C, et al. Ileal bile acid transporter inhibition in Cyp2c70 KO mice ameliorates cholestatic liver injury. J Lipid Res 2022;63:100261.
[20] Kunst RF, de Waart DR, Wolters F, et al. Systemic ASBT inactivation protects against liver damage in obstructive cholestasis in mice. JHEP Rep 2022;4:100573.